Hadronic Final States in $\gamma^* p$ Diffraction

Alice Valkárová
Nuclear Center of Charles University, V Holešovičkách 2, 180 00,Praha 8,
Czech Republic.
(April 24, 1998)

Event shape, charged hadron distributions and multiplicity structure of Large-Rapidity-Gap events have been studied in ep collisions at HERA. Results were compared with results obtained by studying e^+e^- and μp interactions and used to test different models of diffractive production.

I. INTRODUCTION

The kinematics of the Large-Rapidity-Gap (LRG) events can be discussed in terms of the process

$$e(k) \ + \ p(P) \rightarrow e(k') \ + \ X(x) \ + \ Y(P') \tag{1}$$

where hadronic systems X and Y are separated by the largest rapidity gap in the event.

The kinematics are described by the variables $Q^2 = -q^2 = -(k-k')^2$, $t = (q-x)^2 = (P-P')^2$ and $W^2 = (q+P)^2$. The system Y is the final state including the proton. Incoming photon (ranging from low to high virtuality Q^2) can be excited into a vector meson,or can dissociate into a high mass state X. In this paper,the topological structure and hadronic distributions of the final state X is investigated.

The results presented are based upon data recorded by the H1 [1] and ZEUS [2] detectors in 1994 when positrons with energy 27.5 GeV and protons of energy 820 GeV were collided head-on in HERA.

II. EVENT SHAPE ANALYSIS IN DIFFRACTIVE DIS

In the centre of mass of a system X of N particles, the thrust method determines the direction of the unit vector $\vec{a}$ along which the projected momentum flow is maximal [3]. Thrust is computed as [4]:

$$T = (1/\sum_{i=1}^{N} |\vec{p}_i|) \cdot \max_{\vec{a}} \sum_{i=1}^{N} |\vec{p}_i \cdot \vec{a}|$$

where $\vec{p}_i$ represents the momentum of particle i, in the rest frame of the N particles. The N particles are then grouped uniquely into two subsets (thrust jets) with independent masses, and equal but opposite 3-momenta. Thrust values range from a maximum value of $T = 1$ in the case of any collinear configuration, to a minimum value of $T = 0.5$ obtained in an isotropic system X with infinite multiplicity.

A transverse thrust jet momentum P_t can be defined relative to a reference direction $\vec{r}$ (here: the proton beam direction transformed into the centre of mass frame of the system X) as $P_t = P \cdot \sin\Theta$ with Θ being the angle between $\vec{P}_i$ and $\vec{r}$. Since the 4-momentum transfer squared t is small in LRG events with a forward rapidity gap, this direction is a good approximation to the $\gamma^* I\!P$ axis,where $I\!P$ is the exchanged object.

Sphericity is defined as

$$S = 3/2 \cdot \min_{\vec{n}} \sum_{i=1}^{N} p_{Ti}^2 / \sum_{i=1}^{N} p_i^2$$

where $\vec{n} = \vec{n}_3$, $\vec{n}_3$ are the unit vectors of sphericity axis, $\vec{n}_1$ is perpendicular to the event plane. Sphericity $S = 1(0)$ for fully spherical (collinear) configuration.

Event shape of DIS events has been studied by both H1 [5] and ZEUS [6] experiments.

Measurements have been made by H1 (ZEUS) over the range $30(160) < W_{\gamma p} < 210(250)$ GeV, $0(0.04) < y < 0.5(0.95)$ and $10(5) < Q^2 < 100(185)$ GeV^2. A diffractive signal from the H1 data is observed by requiring $M_Y < 1.6$ GeV, $x_{I\!P} < 0.05$ where $x_{I\!P} = (Q^2 + M_X^2)/(Q^2 + W^2)$, and absence of significant activity in forward detectors covering

$7.5 > \eta > 3.2$. In addition, at H1 (ZEUS) $\eta_{max} < 3.2(2.0)$ where η_{max} is the pseudorapidity of the forward most energy cluster in the calorimeter. Using simulated events,the measured distributions for H1 have been fully corrected for detector resolution and acceptance losses to give cross sections in the kinematic region of M_Y,$x_{I\!P}$,Q^2 and y defined above. On the contrary ZEUS measurements are corrected within η_{max} <2.

In Fig.1 thrust is shown as a function of $1/M_X$,averaged in M_X intervals ranging from 4 to 36 GeV together with the available data for thrust in e^+e^- annihilation [7] plotted at $M_X = \sqrt{s_{ee}}$. The slopes are comparable, but $\langle T\rangle$ of DIS LRG events is lower. The cross sections differential in P_t^2 are shown in Fig. 2a for six M_X intervals in the mass range from 6 to 36 GeV, and normalized to unity in each M_X interval. The data show:

- a steep rise of the distribution towards low P_t^2 values, demonstrating a dominant alignment of the final state thrust axis with the initial $\gamma^* p$ collision direction;
- a shape of the P_t^2 distributions nearly independent of M_X, suggesting the factorizable form

$$\mathrm{d}\sigma(M_X, P_t^2)/\mathrm{d}P_t^2 = A(M_X) \cdot B(P_t^2); \qquad (2)$$

- a substantial high P_t^2 tail.

In Fig. 2b, the correlation of $< T >$ with P_t of the system X is presented We observe that events with larger values of P_t have smaller values of $< T >$ corresponding to a less aligned structure of the events compared to the $q\bar{q}$ state. In Fig. 3a the value of thrust is compared with model predictions. In Fig 3b the fractions of events with $P_t^2 > 3$ (GeV)^2 are plotted together with model predictions. The data for sphericity S and thrust T for experiment ZEUS are shown together with prediction of different models in Fig. 4. In all these figures we can see that models where the matrix element is included (RAPGAP RG [8]),LEPTO [9] and VBLY [10] with 2 and 3-jet diagrams) are more close to data than the RAPGAP version of model with $q\bar{q}$ mode only (which corresponds to simple Aligned Jet Model [11]). All models however fail to describe fractions of events with large P_t^2.

All decribed features of HERA data cannot be explained by pure $q\bar{q}$ configuration. Substantial contribution of higher multiplicity configurations (like $q\bar{q}g$) is required in X. This is consistent with the results found in [12].

III. CHARGED TRACKS DISTRIBUTIONS

Charged particle distributions were measured by both H1 [13] and ZEUS [14]. A diffractive signal from the H1 data is observed by requiring the same cuts as in the event shape analysis. For the calorimetric clusters required H1 (ZEUS) $\eta_{max} < 3.0(2.0)$ and in addition, in the ZEUS analysis the cut on polar angle of the hadronic final state was used: $\vartheta_H > 0.75$ rad where $\vartheta_H = arccos(\sum_{i=1}^{N} p_{Z,i}/\sum_{i=1}^{N} E_i)$. The kinematic range studied was for H1 (ZEUS) $0.05(0.04) < y < 0.6(0.85)$, $7.5(7) < Q^2 < 100(160)$ GeV^2, $x_{I\!P} < 0.05$ for H1 and $130 < W < 185$ GeV for ZEUS.

In Fig. 5a,the Feynman x variable $x_F = 2p_l^*/M_x$ for diffractive events [1] is plotted and compared with non-diffractive events in μp interactions [15]. We observe the symmetry between forward and backward hemispheres for diffractive events indicating that exchanged object (pomeron) is not a baryon-type remnant. In Fig 5b, the dependence of $< p_T^2 >$ as a function of x_F ("Seagull plot") is shown for both HERA experiments and compared with non-diffractive μp interactions. Overall, the level of parton radiation effects appears to be much stronger in the diffractive scattering processes compared to the non-diffractive interactions at comparable masses of the hadronic final state.

The distributions of density of charged particles in LRG events are shown for different intervals of M_X in Fig 7 [16]. H1 data are compared with e^+e^- , [17] μp, μD data [15] and model prediction of RAPGAP generator [8]. Particle densities for diffractive data are larger in the central region than for e^+e^- and μN data, the diffractive distributions are more symmetric than non-diffractive ones. This can be explained again by larger gluonic contents of the diffractive hadronic system compared to e^+e^- and μN systems.

[1] For diffractive events M_X plays a role of W of non-diffractive events.

IV. CONCLUSIONS

The abundance of parton multiplicities higher than $q\bar{q}$ implied by properties of diffractive processes in deep inelastic scattering is consistent with the gluon-dominated colour singlet exchange found in QCD-fits [12]. Equivalently, in the proton rest frame,the diffractive processes can be understood as the processes when partonic fluctuations of the virtual photon interact with the target with $N(\gamma^* \to q\bar{q}g\ )/N(\gamma^* \to q\bar{q}\ )$ larger than in e^+e^- or μp interactions.

---

[1] I. Abt et al., H1 Collaboration, Nucl. Inst. Meth. A386 (1997) 310.
[2] The ZEUS Detector, Status Report, DESY (1993).
[3] S. Brandt et al., Phys. Lett. 12 (1964) 57.
[4] E. Farhi, Phys. Rev. Lett. 39 (1977) 1587.
[5] C.Adloff et al., H1 Collaboration, Eur. Phys.J. C1, (1998) 495.
[6] J.Breitweg et al., ZEUS Collaboration, DESY 97-202 (October 1997) accepted by Physics Letters B
[7] PLUTO Collab., Ch. Berger et al., Z. Phys. C12 (1982) 297.
MARK II Collab., A. Peterson et al., Phys. Rev. D37 (1988) 1;
TASSO Collab., W. Braunschweig et al., Z. Phys. C45 (1989) 11 and Z. Phys. C47 (1990) 187
[8] H. Jung, Comp. Phys. Comm. 86 (1995) 147;
H. Jung, "Modelling Diffractive Processes", Topical Conference on Hard Diffractive Processes, Eilat, Israel, Febr. 1996, p. 406.
[9] G. Ingelman, A. Edin, and J. Rathsman, "LEPTO 6.5 - A Monte Carlo Generator for Deep Inelastic Lepton-Nucleon Scattering", DESY 96-057.
[10] J.Vermaseren,F.Barreiro,L.Labarga and F.J.Yndurain DESY 97-031, FTUAM 96-7,accepted by Physics Letters B.
[11] J.D. Bjorken and J.B. Kogut, Phys. Rev. D8 (1973) 1341.
[12] C.Adloff et al., H1 Collaboration, Inclusive Measurements of Diffractive Deep-Inelastic ep Scattering, DESY 97-158,subm. to Z.Phys.C
[13] H1 Collaboration, Paper pa02-062, submitted to the 28th International Conference on High Energy Physics, Warsaw, Poland, July 1996.
[14] ZEUS Collaboration, Paper N-660 PA2/4 PL2/3 submitted to the 28th International Conference on High Energy Physics, Warsaw, Poland, July 1996.
[15] M.Arneodo et al., EMC Collaboration, Z.Phys. C35 (1987) 417.
[16] Abstract 250, submitted to the 29th International Conference on High Energy Physics, Jerusalem, Israel, August 1997.
[17] JETSET 7.3 and 7.4, T. Sjöstrand, Comput. Phys. Com. 82 (1994) 74.

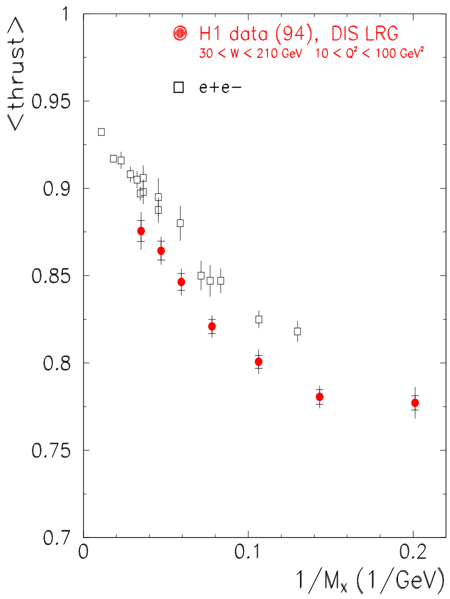

Figure 1: Average thrust $\langle T\rangle$, as a function of $1/M_X$ for LRG data, and for e^+e^- annihilation data [7] as a function of $1/\sqrt{s_{ee}}$

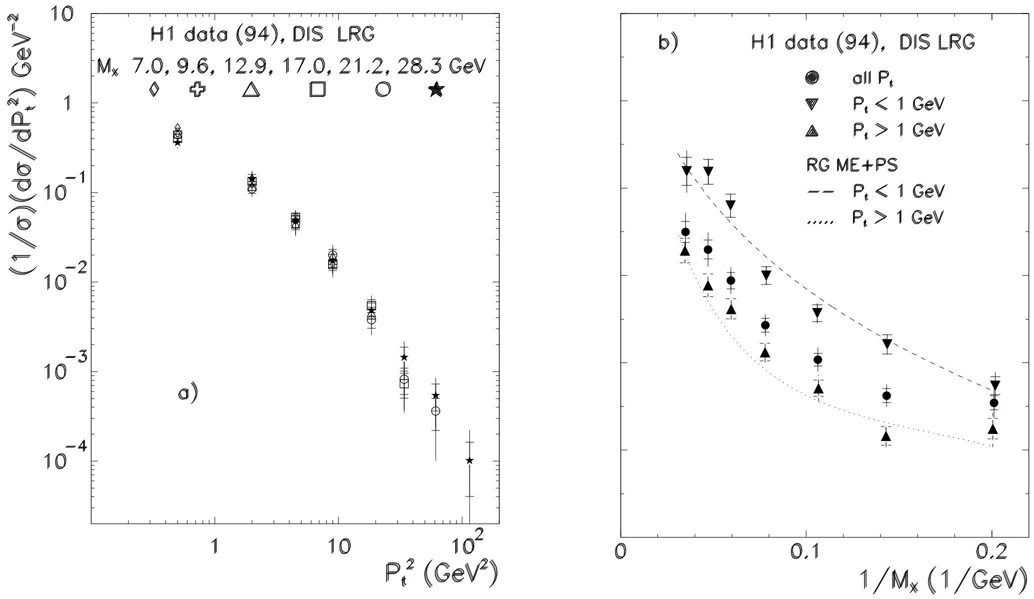

Figure 2a: Normalized thrust jet P_t^2 distributions for six M_X intervals. The P_t^2 bin limits are 0, 1, 3, 6, 12, 25, 43, 79, and 151 GeV^2; **2b:** Average thrust $\langle T\rangle$, as a function of $1/M_X$, for all events, for events with $P_t < 1$ GeV and for events with $P_t > 1$ GeV, with predictions from RAPGAP . The data points are given at $1/\langle M_X\rangle$.

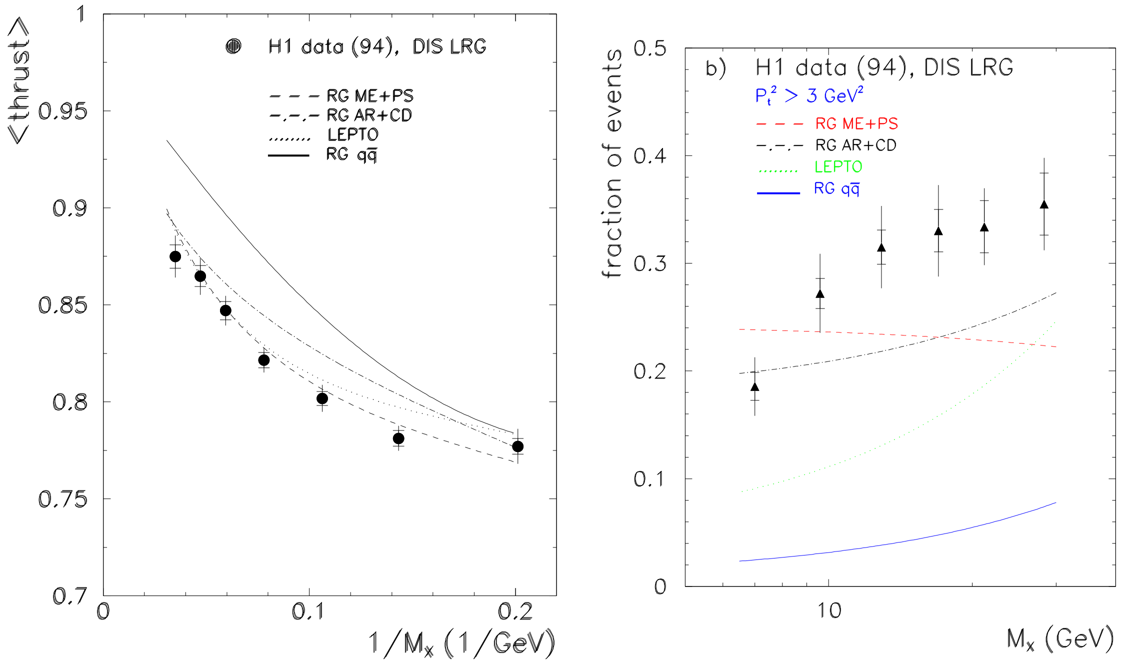

Figure 3a: Comparison of model predictions with the M_X dependence of $\langle T \rangle$. **3b:** Fraction of events with $P_t^2 > 3$ GeV^2 for six M_X intervals, together with four model predictions .

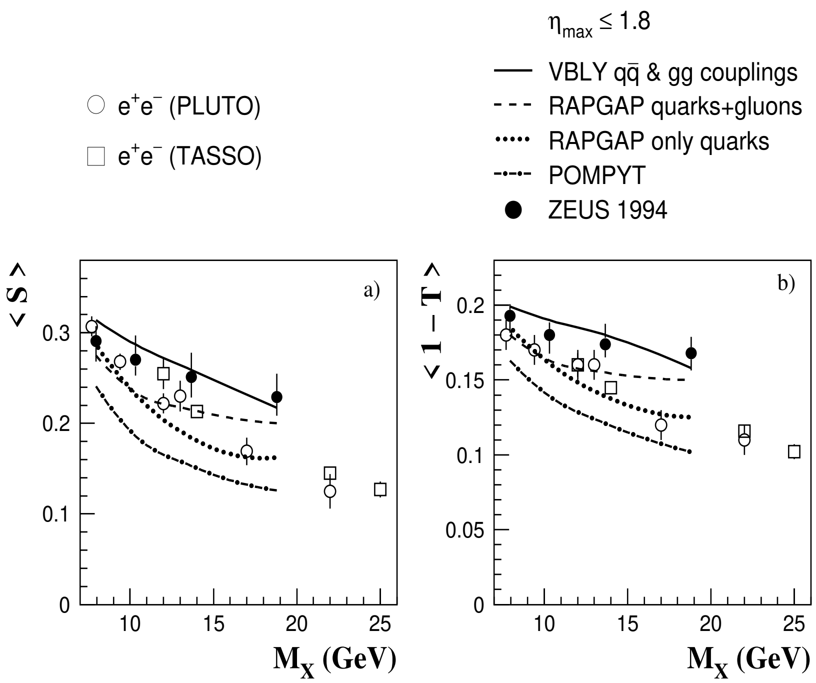

Figure 4: Sphericity and one minus thrust plotted as a function of M_X (ZEUS) compared with model predictions.

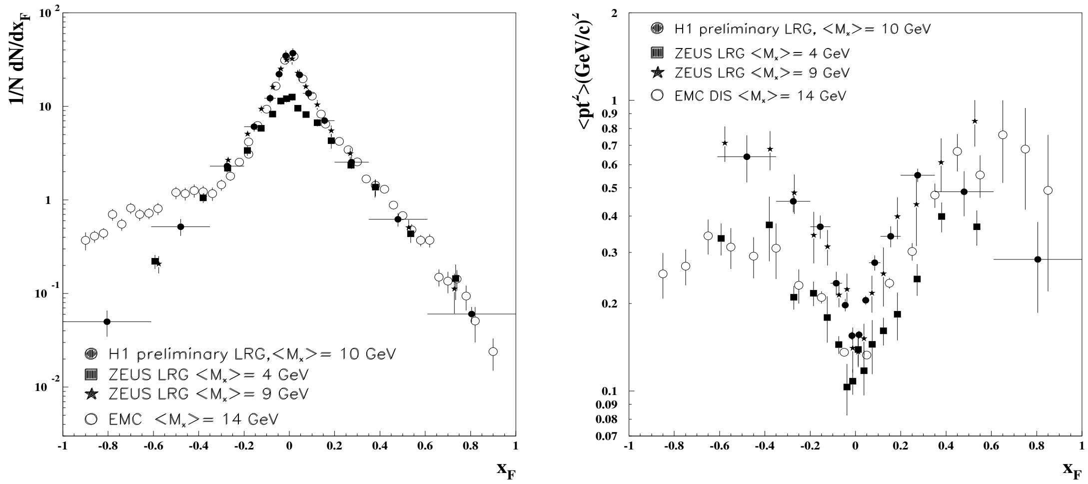

Figure 5a: X_F plot showing fully corrected H1 data and ZEUS data (for $\eta_{max} < 2.$) compared with E.M.C. data. **5b:** Seagull plot showing fully corrected H1 data and ZEUS data (for $\eta_{max} < 2.$) compared with E.M.C. data.

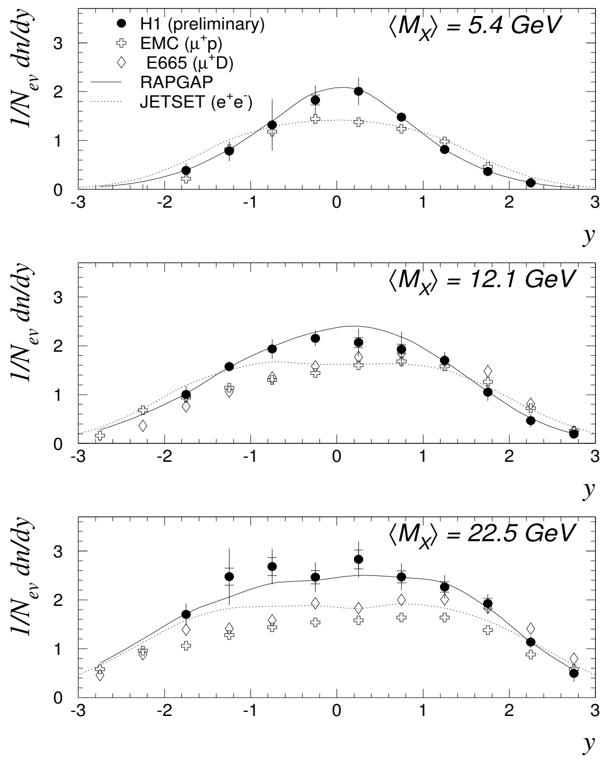

Figure 6: Charged particle rapidity spectra for three intervals in M_X (H1), at W=$< M_X >$ (μN) and at $\sqrt{s_{ee}} =< M_X >$ (JETSET e^+e^- [17]) .